

Light-element and purely charge-based topological materials

Nassim Derriche, Marcel Franz, and George Sawatzky
*Department of Physics and Astronomy & Stewart Blusson Quantum Matter Institute,
University of British Columbia, Vancouver BC, Canada V6T 1Z4*

We examine a class of Hamiltonians characterized by interatomic, interorbital even-odd parity hybridization as a model for a family of topological insulators without the need for spin-orbit coupling. Non-trivial properties of these materials are exemplified by studying the topologically-protected edge states of s - p hybridized alkali and alkaline earth atoms in one and two-dimensional lattices. In 1D the topological features are analogous to the canonical Su-Schrieffer-Heeger model but, remarkably, occur in the absence of dimerization. Alkaline earth chains, with Be standing out due to its gap size and near particle-hole symmetry, are of particular experimental interest since their Fermi energy without doping lies directly at the level of topological edge states. Similar physics is demonstrated to occur in a 2D honeycomb lattice system of s - p bonded atoms, where dispersive edge states emerge. Lighter elements are predicted using this model to host topological states in contrast to spin-orbit coupling-induced band inversion favoring heavier atoms.

The study and search for topologically insulating materials is an important part of contemporary materials science research owing to the unique and often useful properties such systems exhibit. Topological insulators, by definition, host states physically localized on the surfaces or edges of a sample that energetically lie in a gap of the bulk material's band structure [1–3]. Because the emergence of these surface states is rooted in topology and the associated symmetries of the Hamiltonian, their existence can be robustly protected from impurities or external perturbations. This makes topological insulators appealing platforms for various applications such as the low-dissipation semiconductor devices and, due to the spin-momentum locking of surface states, also for magnetic applications [4–7]. A plethora of systems has been shown to be topological insulators but the search for new candidates is ongoing, motivated by the need for specific physical properties and materials suitable for technological applications.

We examine and analyze here a class of Hamiltonians that host topological phases, applicable to materials in which interorbital hybridization of even (*gerade*) and odd (*ungerade*) atomic orbitals is a significant part of the low energy electronic physics. As prototypical examples, we focus on systems dominated by nearest-neighbor sigma hybridization between s and p orbitals; due to their electron configuration, alkali and alkaline earth atoms constitute excellent systems to which our model can be applied. We concentrate on lower-dimensional materials since, compared to 3D systems, they more commonly feature band gaps extending over the full Brillouin Zone. These systems however have different electronic structures and Fermi energies than their 3D counterparts. The fundamental physics of interest for such materials is at first most clearly illustrated in a one-dimensional chain; such a system has been studied in the framework of the modern theory of polarization [8–10], but the aim of the 1D-focused part of this article is to formally describe the topology involved by analyzing a simple Hamiltonian

containing the key even-odd orbital hybridization (similarly to the Shockley model) [11, 12] in order to show that it is enough for topological phases to emerge by using realistic parameters calculated with an *ab initio* approach, specifically density functional theory (DFT) in this work [13, 14].

For materials to exhibit this type of topological behaviour, their band structure needs to feature a gap induced by the avoided crossing of an even and an odd parity band. For this to be of practical importance, their chemical potential should lie in this gap either naturally or by shifting it accordingly through small electron or hole doping. This makes the topologically-protected edge states emerging in the gap experimentally accessible. The alkali and alkaline earth linear chains and 2D honeycomb lattices discussed in detail later feature such gaps. As shown in Table I, while the Fermi energy in the conducting alkali chains is separated from the gap, for alkaline earth chains which have two valence electrons per atom it lies in the gap and, additionally, directly at the energy of the degenerate edge states E_{Edge} in the topological phase [15]. Consequently, we present data focused more on the alkaline earth materials in this work. Of course, there are likely alloys and intermetallic compounds in which these elements play a dominant role in the valence electronic structure where this also could occur, highlighting the rather broad classes of materials that potentially exhibit this type of topological behavior. Naturally, the discussion of a topological insulator involving p orbitals brings graphene to mind as a historically important system [16–18]. The model ingredients we consider here are however fundamentally different and spinless; proposals for graphene-based [19, 20] and even 2D trigonal s - p topological insulators [21] are characterized by the rise of the quantum spin Hall effect that requires strong spin-orbit coupling, whose strength is increased through the adsorption of heavy atoms or a substantial external field [22].

We consider a one-dimensional infinite chain of equidis-

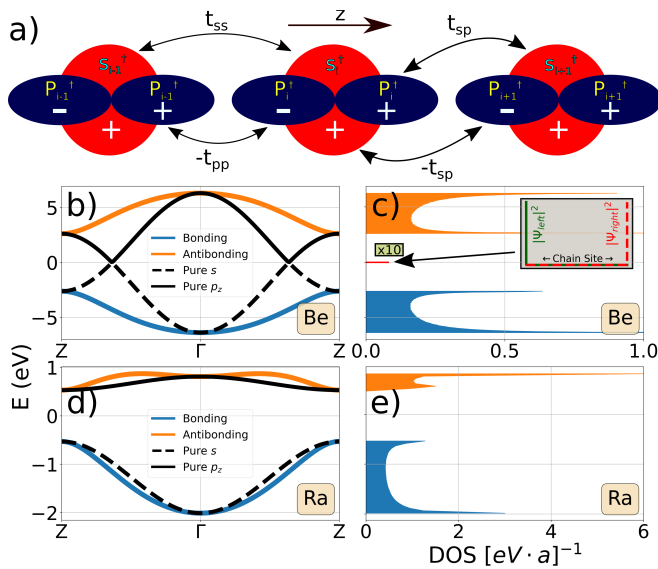


FIG. 1. s - p chain results. a) Diagram of a uniform chain of s and p orbitals and the allowed nearest-neighbor hopping processes. b) Band structure calculated with Eq. (1) (black curves have $t_{sp} = 0$ structure). The high symmetry points are Γ ($k = 0$) and Z ($k = \pm \frac{\pi}{2a}$). c) Density of states of a $N = 5000$ chain of Be atoms, where the value for the edge states in red has been multiplied by 10 for visual clarity. Inset: charge density of the two degenerate edge states in the gap. d) and e) are the same as b) and c) for Ra chains which don't exhibit gap states. The Fermi energy is set at $E = 0$, and the *ab initio* parameters used are listed in Table I.

tant atoms that each host an s orbital and a p orbital with lobes aligned along the chain axis, as illustrated in Fig. 1 (a). The tight binding Hamiltonian in reciprocal space in an ordered (s, p) basis reads

$$h(k) = \begin{pmatrix} -2t_{ss} \cos(ak) - \frac{\Delta}{2} & -2it_{sp} \sin(ak) \\ 2it_{sp} \sin(ak) & 2t_{pp} \cos(ak) + \frac{\Delta}{2} \end{pmatrix}, \quad (1)$$

where Δ is the on-site energy difference between the p and s orbitals in the chain, a is the lattice constant and k represents the crystal momentum in the chain direction [23]. In Fig. 1 (b) and (d), the band structure using beryllium and radium parameters listed in Table I respectively are displayed. Comparing the bands with ($t_{sp} > 0$) and without ($t_{sp} = 0$) s - p mixing in Fig. 1 shows that the light Be chain bands in (b) anticross, leading to the manifestation of two degenerate edge states in the gap in (c), while the heavy Ra chain in (d) has no crossing at all and thus no topological states in (e). We note that the p_x and p_y orbitals, which are higher in energy from the chain-aligned p_z orbitals by crystal field effects, are not important to this model [15]. The two alkaline earth extremes were selected to highlight and contrast the mass dependence of the s - p hybridization topological phenomenon with the more common spin-orbit coupling induced topology. As shown in the gap data found in Table I, the lighter elements host topological phases and

the band gap monotonically decreases for alkali and alkaline earth materials respectively until the gap closes, indicating a transition from the topological to the trivial phase in which no avoided crossing occurs, and then the gap increases monotonically. On the other hand, the strength of relativistic effects, including spin-orbit coupling, increases strongly with higher nuclear charge and principal quantum number n of the valence band states [24–26]. This, along with the decrease of the bandwidths with nuclear charge controlled by t_{ss} and t_{pp} due to larger equilibrium lattice constants a and the increasing emergence of nodes in the orbital wavefunctions affecting orbital overlaps, explains why heavier elements exhibit increased separation between ns and np bands thus avoiding band crossing in the first place [27].

Element	a	Δ	t_{ss}	t_{pp}	t_{sp}	1D		2D	
						E_{Edge}	Gap	E_{Edge}	Gap
Li	3.04	2.64	1.19	1.51	1.36	2.54	2.75	3.81	3.19
Be	2.15	3.73	2.25	2.23	2.35	0.00	5.23	2.61	6.36
Na	3.28	4.57	1.03	1.69	1.31	2.17	0.87	4.43	1.09
Mg	3.07	4.96	1.04	1.70	1.31	0.00	0.53	1.01	0.78
K	4.10	2.73	0.65	0.84	0.74	1.32	0.27	2.68	0.52
Ca	3.99	2.12	0.58	0.34	0.55	-	0.28	0.20	0.18
Rb	4.34	2.19	0.56	0.43	0.57	-	0.22	2.30	0.19
Sr	4.48	1.75	0.47	0.12	0.43	-	0.57	-	0.18
Cs	4.76	1.68	0.46	0.16	0.40	-	0.43	-	0.09
Ba	3.90	2.25	0.63	0.01	0.40	-	0.98	-	0.36
Fr	4.69	2.40	0.49	0.30	0.41	-	0.83	-	0.50
Ra	5.11	1.94	0.37	0.07	0.32	-	1.04	-	0.71

TABLE I. Topological phase data of 1D chains and 2D honeycomb lattice alkali and alkaline earth materials. The results are based on the listed Hamiltonian parameters, which were obtained from fits to *ab initio* calculations performed using FPLO, an atomic orbital-based DFT code [28]. E_{Edge} is the energy of the center of topological edge states in the gap with respect to the Fermi energy set to zero. All energies are given in eV, and the equilibrium lattice constants a are in angstrom.

As is convenient for the topological analysis of two-band systems, we write the Hamiltonian (1) as $h(k) = d_0(k)\sigma_0 + \mathbf{d}(k) \cdot \boldsymbol{\sigma}$ in terms of a vector $\boldsymbol{\sigma} = (\sigma_x, \sigma_y, \sigma_z)$ of Pauli matrices acting in the orbital (s, p) basis and the identity matrix σ_0 . Here $d_0(k) = -2t_- \cos(ak)$,

$$\mathbf{d}(k) = (0, 2t_{sp} \sin(ak), -2t_+ \cos(ak) - \Delta/2), \quad (2)$$

and $t_{\pm} = (t_{pp} \pm t_{ss})/2$. For generic values of parameters $h(k)$ respects spinless time-reversal symmetry $\mathcal{T} : h(k)^* = h(-k)$ with $\mathcal{T}^2 = 1$, which places it in class AI of the Altland-Zirnbauer classification [29]. In space dimensions 1 and 2 this class allows only trivial topology and hence we do not expect any strong topological phases in our model. If, however, we include spatial symmetries, then weak topological phases become possible.

The Hamiltonian (1) is inversion-symmetric, respecting $\mathcal{I} : \sigma_z h(k) \sigma_z = h(-k)$. The two symmetries, \mathcal{T} and \mathcal{I} , together enforce the absence of the σ_x term in $h(k)$, as also manifest in Eq. (2). This form of Hamiltonian implies a quantized winding number,

$$\gamma_C = \frac{1}{2\pi i} \int_{-\pi/a}^{\pi/a} dk \langle u(k) | \partial_k | u(k) \rangle, \quad (3)$$

where $u(k)$ denotes the periodic part of the Bloch wavefunction of the occupied band. For a 2×2 Bloch Hamiltonian $4\pi\gamma_C$ equals the solid angle swept out by $\mathbf{d}(k)$ as k traverses the Brillouin zone. When $\mathbf{d}(k)$ is confined to a plane as is enforced here by the presence of the inversion symmetry, only $\gamma_C = 0, \pm 1/2$ are possible which respectively correspond to a trivial and topological phase. The Hamiltonian (1) thus possesses a Z_2 topological invariant and is topologically equivalent to the SSH model [30–32].

The main physical aspect distinguishing the topological from the trivial regime is that the band structure in the topological phase is highly s - p hybridized, while the trivial phase is reached if the energy difference between the s and p levels is high enough such that no avoided crossing occurs between the upper and the lower band. This contrasts these systems from the dimerization-driven SSH model. However, this essential behavior would be absent if not specifically for the even-odd nature of that hybridization, which can be visualized in Fig. 1 (a) as s - p hopping to the left and to the right of a given site having opposite signs. If, for example, we replaced the p orbital by another of the same energy but with even parity, the off-diagonal terms in the Hamiltonian (1) would not be of the form $\pm i \sin(ak)$ thus removing the possibility of a non-zero winding number around the origin in the Pauli matrix space. The Kitaev chain Hamiltonian has exactly the same off-diagonal element structure (in that case due to the form of the p -wave superconducting order parameter). Systems involving higher angular momentum states than s or p can also have even-odd mixing symmetry, similarly making them potential candidates for extending the reach of this mechanism to other classes of materials. Interesting candidates would be ones involving p and d bands, or f and d bands [33] which often also involve strong correlations and magnetic phases [34].

For systems with inversion symmetry and a Z_2 topological classification, it is possible to calculate the invariant by analyzing the inversion properties of the eigenstate representing the occupied fermionic band, in our case the lower, mainly s band. We thus express the k -dependent wavefunction $\Psi(k)$ associated with this band as

$$\Psi(k) = \alpha_s(k)\phi_s + \alpha_p(k)\phi_p, \quad (4)$$

where ϕ_s and ϕ_p are the wavefunctions associated with the s and p atomic states respectively, and $\alpha_s(k)$ and

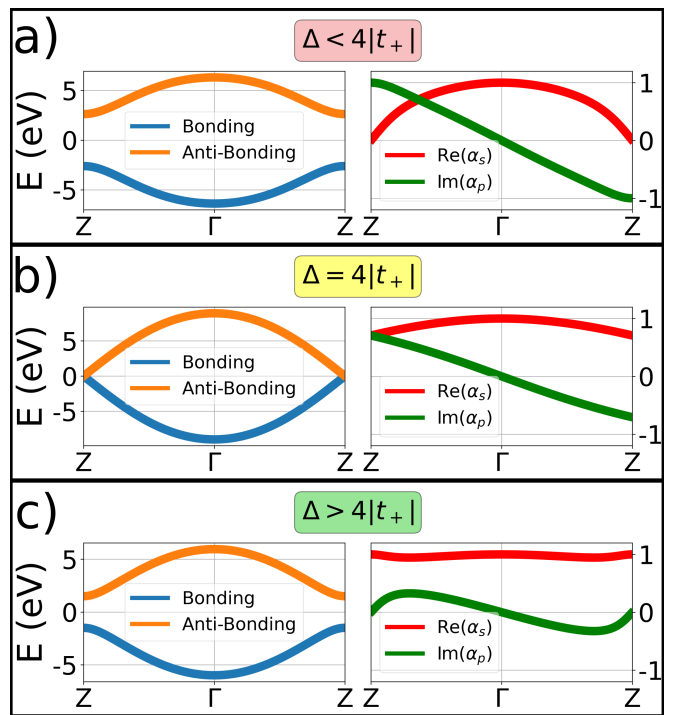


FIG. 2. 1D chain band structure (left column) and the eigenstates of the lower band with respect to k (right column) in different regimes; a) for the topological phase, b) at the phase transition point and c) in the trivial regime. The Fermi energy is set at $E = 0$, and $t_{sp} > 0$ for all cases.

$\alpha_p(k)$ are normalized complex coefficients. With a suitable choice for the overall phase, we can write this wavefunction such that $\alpha_s(k)$ is purely real and $\alpha_p(k)$ is purely imaginary for all k [23]. Then, if we consider the eigenvalue $\gamma(k)$ of the inversion operator \mathcal{I} associated with $\Psi(k)$ at the two special k -points that map to themselves under inversion, namely $k = 0$ and $k = \frac{\pi}{a}$, we can define a Z_2 invariant ν as

$$\nu = \gamma(0)\gamma\left(\frac{\pi}{a}\right). \quad (5)$$

In this case, $\gamma(k)$ can only be equal to 1 or -1 . Thus, ν also either has the value 1 (trivial phase, $\Delta > 4|t_+|$) or -1 (topological phase, $\Delta < 4|t_+|$ and $t_{sp} > 0$) [35, 36]. This is consistent with the results displayed in Fig. 2; for the topological phase, $\gamma(0) = 1$ and $\gamma(\frac{\pi}{a}) = -1$, while they are both equal to 1 for the trivial phase. At exactly the phase transition point $\Delta = 4|t_+|$ the winding number is undefined since the system becomes gapless and it is not possible to uniquely identify the eigenstate belonging to the lower band. It is crucial to note here that the band structures in (a) and (c) are nearly identical in shape and structure. Consequently, looking solely at DFT band structures, one may not recognize that a system is in a topological phase; information about the electronic wavefunctions is necessary. Seeking only band crossings with Dirac-like dispersion and spin-orbit degen-

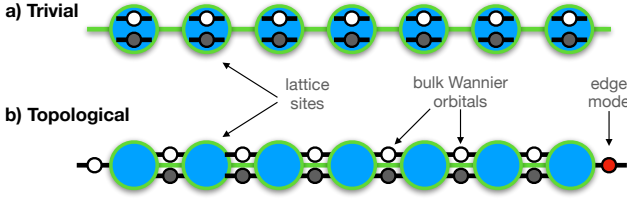


FIG. 3. Physical origin of the fractionally quantized polarization in the s - p chain with N sites. a) The trivial phase ($\gamma_C = 0$), where N Wannier orbitals are centered at the lattice sites. b) The topological phase ($\gamma_C = \pm \frac{1}{2}$), where $N - 1$ Wannier centers are located midway between the lattice sites, forcing an electron to occupy one of two edge modes resulting in polarization $P = \pm \frac{e}{2}$.

eracy breaking, the type of topology highlighted here can easily be missed.

In the special case $t_{pp} = t_{ss}$, the term in $h(\mathbf{k})$ proportional to σ_0 vanishes and the Hamiltonian acquires particle-hole symmetry, $\mathcal{P} : \sigma_x h(\mathbf{k})^* \sigma_x = -h(-\mathbf{k})$ with $\mathcal{P}^2 = 1$. This places the system in class BDI which admits integer topological classification in 1D [37]. The Hamiltonian then becomes topologically equivalent to the Kitaev chain where the topological invariant counts the number of Majorana zero modes localized at one end of the chain [38–40]. In our case the Hamiltonian acts in the space of s and p orbitals (and not in Nambu space) but zero modes still form when in the topological phase. The fact that the Be chains almost exhibit this symmetry since $t_{ss} \approx t_{pp}$ as seen in Table I highly increases the potential for experimental observation of its topological edge states since their centering in the large band gap shown in Fig. 1 (c) makes it harder for perturbations to shift their energy up or down which would lead to them being swallowed by the bulk bands. Like in the SSH model, the physical observable associated with the topological phase are the two fractional polarization states $P = \pm \frac{e}{2}$ which can be interpreted as the last valence electron residing in one of the two degenerate end modes [41]. An intuitive picture for this mechanism is given in Fig. 3, which shows the emergence of edge Tamm states in the topological phase [42, 43].

While physically enlightening, one-dimensional models are often difficult to realize experimentally although we here envision the possibility of forming 1D chains at step edges of a substrate which is inert regarding covalent interactions with the chain atoms [44]. We thus extend our analysis by considering a 2D honeycomb lattice governed by the same even-odd interatomic hybridization and demonstrate that the conclusions we reached for the 1D system also apply in higher dimensions. The honeycomb lattice was specifically chosen because, in analogy with graphene, its energy spectrum is gaped for all \mathbf{k} away from two Dirac points and can be easily turned insulating. This is unlike most square lattice systems

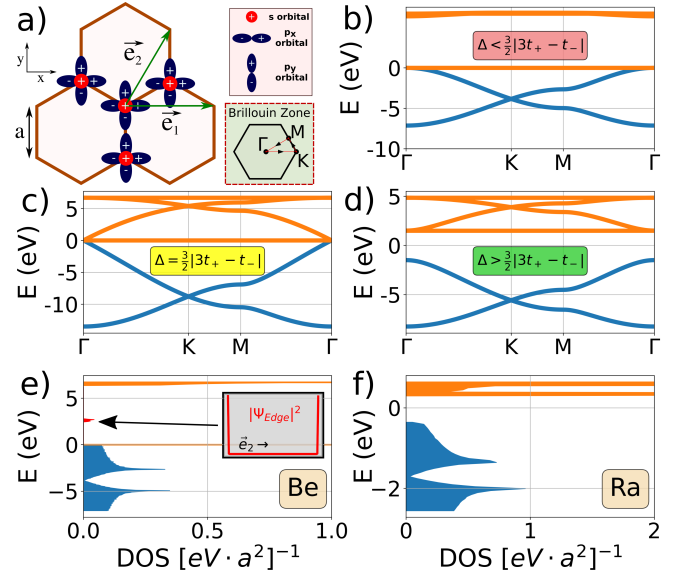


FIG. 4. Results for a 2D s - p honeycomb lattice. a) Honeycomb lattice with an s , p_x and p_y orbital at each site. \vec{e}_1 and \vec{e}_2 are the primitive lattice vectors, and high symmetry points in the associated Brillouin Zone are shown. b) Band structure in the topological phase, c) at the phase transition point and d) in the trivial phase. e) Density of states of a honeycomb strip that is infinite along the \vec{e}_1 direction with a thickness of 100 unit cells in the \vec{e}_2 direction made of Be atoms, and f) of Ra atoms. The inset shows the momentum-averaged combined charge density of the two gap topologically protected dispersive edge modes. The Fermi energy is set at $E = 0$.

which typically exhibit large Fermi surfaces, distinguishing this system from the BHZ model [1, 45]. As shown in Fig. 4 (a), each site of the honeycomb lattice in the x - y plane hosts an s , p_x and p_y orbital, and nearest neighbor hopping between all of those is allowed. The resulting 6-band Hamiltonian is most easily written in the chiral basis ($s_A, p_{A+}, p_{A-}; s_B, p_{B+}, p_{B-}$) where s_η denotes the s orbital on $\eta = A, B$ sublattice and $p_{\eta\pm} = p_{\eta\pm} \pm ip_{\eta y}$. It reads

$$h(\vec{\mathbf{k}}) = \begin{pmatrix} h_0 & h_{AB}(\vec{\mathbf{k}}) \\ h_{AB}(\vec{\mathbf{k}})^\dagger & h_0 \end{pmatrix}, \quad (6)$$

where $h_0 = \text{diag}(-\Delta, \Delta, \Delta)/2$,

$$h_{AB}(\vec{\mathbf{k}}) = \begin{pmatrix} t_{ss}z_0(\vec{\mathbf{k}}) & t_{sp}z_2(\vec{\mathbf{k}}) & t_{sp}z_1(\vec{\mathbf{k}}) \\ t_{sp}z_1(\vec{\mathbf{k}}) & t_{pp}z_0(\vec{\mathbf{k}}) & t_{sp}z_1(\vec{\mathbf{k}}) \\ t_{sp}z_2(\vec{\mathbf{k}}) & t_{sp}z_2(\vec{\mathbf{k}}) & t_{pp}z_0(\vec{\mathbf{k}}) \end{pmatrix}, \quad (7)$$

and $z_\mu(\vec{\mathbf{k}}) = e^{i\vec{\mathbf{k}} \cdot \vec{\mathbf{a}}_1} + e^{i\vec{\mathbf{k}} \cdot \vec{\mathbf{a}}_2 - \mu \frac{2\pi}{3}} + e^{i\vec{\mathbf{k}} \cdot \vec{\mathbf{a}}_3 + \mu \frac{2\pi}{3}}$. Here $\vec{\mathbf{a}}_1 = a\hat{\mathbf{y}}$, $\vec{\mathbf{a}}_{2,3} = a(-\sqrt{3}\hat{\mathbf{x}} \pm \hat{\mathbf{y}})/2$ are three nearest neighbor vectors in the honeycomb lattice [17, 46].

Using again the parameters in Table I (with the p_x and p_y atomic levels being degenerate), we compare the band structure in Figs. 4 (b-d). Interestingly, along with lower energy mainly s bands and higher energy mainly

p bands, two completely flat purely p bands appear. We identify these as linear combinations of localized p states in the honeycomb bulk discussed previously [47, 48]. It is interesting to note that the flatness of these bands is not perturbed by the introduction of s - p mixing into the model. Such flat bands are appealing due to their propensity to form strongly correlated phases in the presence of interactions and have been studied in optical and electronic systems [49]. An interesting feature of the Hamiltonian described by Equations 6 and 7 is that, similarly to the 1D chain, a band inversion that occurs when $\Delta = 3|t_{ss} + \frac{t_{pp}}{2}| = \frac{3}{2}|3t_+ - t_-|$. As illustrated in Fig. 4 (b-d), at the phase transition three bands become degenerate at the Γ point whereby the lower flat band detaches from p -bands and attaches to s -bands. Consequently, the Fermi energy for half-filled alkaline earth chains in the topological phase lies right under this set of localized p states, which have to be filled to access the topological end modes in the gap. By projecting the Hamiltonian (6) onto the degenerate subspace it is straightforward to derive an effective 3-band $\vec{k} \cdot \vec{p}$ Hamiltonian for this transition,

$$h_{\text{eff}}(\vec{k}) = \begin{pmatrix} 0 & 0 & -vk_- \\ 0 & 0 & vk_+ \\ -vk_+ & vk_- & m \end{pmatrix}. \quad (8)$$

Here $k_{\pm} = k_x \pm ik_y$, $v = 3t_{sp}a/2$ and $m = \Delta - \frac{3}{2}|3t_+ - t_-|$. The energy eigenvalues are $(m, \pm\sqrt{m^2 + v^2k^2})$. At the transition point marked by $m = 0$ the spectrum consists of a Dirac cone and a flat band, both centered at zero energy. Although once again there is in general no strong topology allowed in the Hamiltonian belonging to AI symmetry class in 2D, we can understand the emergence of the edge modes by regarding the 2D Bloch Hamiltonian $h(k_x, k_y)$ placed on a long strip as a collection of 1D Hamiltonians $h_{k_y}(k_x)$ parametrized by the transverse momentum k_y . We find that, when the system resides in the inverted regime, the flat band contributes a quantized winding number γ_C for each transverse momentum k_y and the invariant ν defined in Eq. (5) is equal to -1 . Like in the 1D chain case, this results in a localized end mode with the energy inside the gap for each k_y . These end modes then form a dispersive edge state visible in Fig. 4 (e). Note that as $h_{k_y}(k_x)$ is not particle-hole symmetric we do not expect the dispersive edge modes to be centered in the gap.

These results open the way for experimental studies of an underexplored type of topological materials favoring lighter elements in contrast to spin-orbit coupling driven topological systems; any material that exhibits the requisite s - p hybridization in its low-energy sector such as the alkali and alkaline earth elements is a potential candidate for the observation of these properties. Notably, due to naturally hosting one more valence electron per atom than the alkali, alkaline earth materials

are of particular interest since their Fermi energy in 1D chains lies directly at the topologically-protected edges modes, making their experimental detection significantly easier. Beryllium chains in particular stand out as the most promising even-odd hybridisation-based topological insulators because of their near particle-hole symmetry and large band gaps strongly protecting the end modes from perturbations compared to other candidates [15]. Beryllene, The 2D honeycomb Be system, has been experimentally realized [50] and would be an excellent system to explore the ramifications of our model, especially since Be-based materials such as Be_3X_2 ($X = \text{C}, \text{Si}, \text{Ge}, \text{Sn}$) [51] have been predicted to be Dirac semimetals and to possess significant contributions from surface states to the density of states at the Fermi energy [52, 53]. Other low-dimensional candidates to explore s - p topological physics which include alkaline earth elements are CaB_6 nanowires [54] or MgB_2 [55].

This research was undertaken thanks in part to funding from the Max Planck-UBC-UTokyo Center for Quantum Materials and the Canada First Research Excellence Fund, Quantum Materials and Future Technologies Program, as well as by the Natural Sciences and Engineering Research Council (NSERC) for Canada.

-
- [1] M. Z. Hasan and C. L. Kane, Reviews of Modern Physics **82**, 3045 (2010), ISSN 0034-6861, URL <https://link.aps.org/doi/10.1103/RevModPhys.82.3045>.
 - [2] X.-L. Qi and S.-C. Zhang, Reviews of Modern Physics **83**, 1057 (2011), publisher: American Physical Society, URL <https://link.aps.org/doi/10.1103/RevModPhys.83.1057>.
 - [3] Marcel Franz and Laurens Molenkamp, *Topological Insulators*, vol. 6 of *Contemporary Concepts of Condensed Matter Science* (Elsevier, 2013), ISBN 978-0-444-63314-9, URL <https://www.sciencedirect.com/bookseries/contemporary-concepts-of-condensed-matter-science/vol/6/suppl/C>.
 - [4] W. Tian, W. Yu, J. Shi, and Y. Wang, Materials **10**, 814 (2017), ISSN 1996-1944, URL <http://www.mdpi.com/1996-1944/10/7/814>.
 - [5] J. Tang, L.-T. Chang, X. Kou, K. Murata, E. S. Choi, M. Lang, Y. Fan, Y. Jiang, M. Montazeri, W. Jiang, et al., Nano Letters **14**, 5423 (2014), ISSN 1530-6984, URL <https://pubs.acs.org/doi/10.1021/nl5026198>.
 - [6] J. Chang, L. F. Register, and S. K. Banerjee, Journal of Applied Physics **112**, 124511 (2012), ISSN 0021-8979, URL <http://aip.scitation.org/doi/10.1063/1.4770324>.
 - [7] W. G. Vandenberghe and M. V. Fischetti, in *2014 IEEE International Electron Devices Meeting (IEEE, 2014)*, pp. 33.4.1–33.4.4, ISBN 978-1-4799-8001-7, URL <http://ieeexplore.ieee.org/document/7047162/>.
 - [8] J. v. d. Brink, Ph.D. thesis, Groningen (1997), URL <https://research.rug.nl/files/3209382/c5.pdf>.
 - [9] G. Brocks, J. van den Brink, and A. F. Morpurgo, Physical Review Letters **93**, 146405 (2004), ISSN 0031-

- 9007, URL <https://journals.aps.org/prl/abstract/10.1103/PhysRevLett.93.146405>.
- [10] N. A. Spaldin (2012), arXiv: 1202.1831, URL <http://dx.doi.org/10.1016/j.jssc.2012.05.010>.
- [11] W. Shockley, *Physical Review* **56**, 317 (1939), publisher: American Physical Society, URL <https://link.aps.org/doi/10.1103/PhysRev.56.317>.
- [12] J.-N. Fuchs and F. Piéchon, *Physical Review B* **104**, 235428 (2021), ISSN 2469-9950, URL <https://journals.aps.org/prb/abstract/10.1103/PhysRevB.104.235428>.
- [13] K. N. Kudin, R. Car, and R. Resta, *The Journal of Chemical Physics* **127**, 194902 (2007), ISSN 0021-9606, URL <http://aip.scitation.org/doi/10.1063/1.2799514>.
- [14] D. Vanderbilt and R. D. King-Smith, *Physical Review B* **48**, 4442 (1993), ISSN 0163-1829, URL <https://link.aps.org/doi/10.1103/PhysRevB.48.4442>.
- [15] A. W. Huran, N. Ben Amor, S. Evangelisti, S. Hoyau, T. Leininger, and V. Brumas, *The Journal of Physical Chemistry A* **122**, 5321 (2018), ISSN 1089-5639, publisher: American Chemical Society, URL <https://doi.org/10.1021/acs.jpca.7b12187>.
- [16] C. L. Kane and E. J. Mele, *Physical Review Letters* **95**, 226801 (2005), ISSN 0031-9007, URL <https://link.aps.org/doi/10.1103/PhysRevLett.95.226801>.
- [17] G. W. Semenoff, *Physical Review Letters* **53**, 2449 (1984), publisher: American Physical Society, URL <https://link.aps.org/doi/10.1103/PhysRevLett.53.2449>.
- [18] A. H. Castro Neto, F. Guinea, N. M. R. Peres, K. S. Novoselov, and A. K. Geim, *Reviews of Modern Physics* **81**, 109 (2009), publisher: American Physical Society, URL <https://link.aps.org/doi/10.1103/RevModPhys.81.109>.
- [19] A. F. Young, J. D. Sanchez-Yamagishi, B. Hunt, S. H. Choi, K. Watanabe, T. Taniguchi, R. C. Ashoori, and P. Jarillo-Herrero, *Nature* **505**, 528 (2014), ISSN 0028-0836, URL <http://www.nature.com/articles/nature12800>.
- [20] D. A. Abanin, P. A. Lee, and L. S. Levitov, *Physical Review Letters* **96**, 176803 (2006), ISSN 0031-9007, URL <https://link.aps.org/doi/10.1103/PhysRevLett.96.176803>.
- [21] Z. F. Wang, K.-H. Jin, and F. Liu, *Nature Communications* **7**, 12746 (2016), ISSN 2041-1723, URL <https://www.nature.com/articles/ncomms12746>.
- [22] I. I. Klimovskikh, M. M. Otrokov, V. Y. Voroshnin, D. Sostina, L. Petaccia, G. Di Santo, S. Thakur, E. V. Chulkov, and A. M. Shikin, *ACS Nano* **11**, 368 (2017), ISSN 1936-0851, URL <https://pubs.acs.org/doi/10.1021/acsnano.6b05982>.
- [23] N. Derriche, I. Elfimov, and G. Sawatzky, *Physical Review B* **106**, 064102 (2022), publisher: American Physical Society, URL <https://link.aps.org/doi/10.1103/PhysRevB.106.064102>.
- [24] E. M. Lifshitz, V. B. Berestetski, L. P. Pitaevskii, J. B. Sykes, and J. S. Bell, *Course of Theoretical Physics, vol. 4.1&2 - Quantum Electrodynamics - Part. 1 & 2*, vol. 4.1&2 (Butterworth-Heinemann, 1971), ISBN 0-08-026503-0 0-08-026504-9, URL <https://www.biblio.com/book/course-theoretical-physics-vol-4-quantum/d/1038026055>.
- [25] H. Tatewaki, S. Yamamoto, and Y. Hatano, *ACS Omega* **2**, 6072 (2017), ISSN 24701343, URL <https://pubs.acs.org/doi/10.1021/acsomega.7b00802>.
- [26] J. Autschbach, *The Journal of Chemical Physics* **136**, 150902 (2012), ISSN 0021-9606, URL <http://aip.scitation.org/doi/10.1063/1.3702628>.
- [27] W. A. Harrison, *Electronic Structure and the Properties of Solids* (Dover Publications, New York, 1989), URL <https://store.doverpublications.com/products/9780486660219>.
- [28] K. Koepnik and H. Eschrig, *Physical Review B* **59**, 1743 (1999), ISSN 0163-1829, URL <https://link.aps.org/doi/10.1103/PhysRevB.59.1743>.
- [29] A. Altland and M. R. Zirnbauer, *Physical Review B* **55**, 1142 (1997), publisher: American Physical Society, URL <https://link.aps.org/doi/10.1103/PhysRevB.55.1142>.
- [30] W. P. Su, J. R. Schrieffer, and A. J. Heeger, *Physical Review Letters* **42**, 1698 (1979), ISSN 00319007, URL <https://journals.aps.org/prl/abstract/10.1103/PhysRevLett.42.1698>.
- [31] E. J. Meier, F. A. An, and B. Gadway, *Nature Communications* **7**, 13986 (2016), ISSN 2041-1723, URL <http://www.nature.com/articles/ncomms13986>.
- [32] A. J. Heeger, S. Kivelson, J. R. Schrieffer, and W. P. Su, *Reviews of Modern Physics* **60**, 781 (1988), publisher: American Physical Society, URL <https://link.aps.org/doi/10.1103/RevModPhys.60.781>.
- [33] K. Zhao, X. Chen, Z. Wang, J. Liu, J. Wu, C. Xi, X. Lv, L. Li, Z. Zhong, and P. Gegenwart, *Physical Review B* **107**, L081112 (2023), publisher: American Physical Society, URL <https://link.aps.org/doi/10.1103/PhysRevB.107.L081112>.
- [34] F. C. Zhang and T. M. Rice, *Physical Review B* **37**, 3759 (1988), ISSN 01631829, URL <https://journals.aps.org/prb/abstract/10.1103/PhysRevB.37.3759>.
- [35] L. Fu and C. L. Kane, *Physical Review B* **76**, 045302 (2007), ISSN 1098-0121, URL <https://link.aps.org/doi/10.1103/PhysRevB.76.045302>.
- [36] A. M. Turner, Y. Zhang, R. S. K. Mong, and A. Vishwanath, *Physical Review B* **85**, 165120 (2012), ISSN 1098-0121, URL <https://link.aps.org/doi/10.1103/PhysRevB.85.165120>.
- [37] A. Kitaev, V. Lebedev, and M. Feigel'man, in *AIP Conference Proceedings* (AIP, 2009), pp. 22–30, URL <http://aip.scitation.org/doi/abs/10.1063/1.3149495>.
- [38] A. Y. Kitaev, *Physics-Uspekhi* **44**, 131 (2001), ISSN 1468-4780, URL <https://iopscience.iop.org/article/10.1070/1063-7869/44/10S/S29>.
- [39] N. Leumer, M. Marganska, B. Muralidharan, and M. Grifoni, *Journal of Physics: Condensed Matter* **32**, 445502 (2020), ISSN 0953-8984, URL <https://iopscience.iop.org/article/10.1088/1361-648X/ab8bf9>.
- [40] M. Leijnse and K. Flensberg, *Semiconductor Science and Technology* **27**, 1 (2012), ISSN 02681242, arXiv: 1206.1736, URL <https://iopscience.iop.org/article/10.1088/0268-1242/27/12/124003>.
- [41] R. Resta, *Reviews of Modern Physics* **66**, 899 (1994), publisher: American Physical Society, URL <https://link.aps.org/doi/10.1103/RevModPhys.66.899>.
- [42] I. Tamm, *Zeitschrift fur Physik* **76**, 849 (1932), ISSN 1434-6001, URL <http://link.springer.com/10.1007/BF01341581>.
- [43] C. A. Downing and L. Martín-Moreno, *Nanophotonics* **10**, 513 (2020), ISSN 2192-8614, URL

- <https://www.degruyter.com/document/doi/10.1515/nanoph-2020-0370/html>.
- [44] H. Xu, S. Liu, Z. Ding, S. J. R. Tan, K. M. Yam, Y. Bao, C. T. Nai, M.-F. Ng, J. Lu, C. Zhang, et al., *Nature Communications* **7**, 12904 (2016), ISSN 2041-1723, publisher: Nature Publishing Group, URL <https://www.nature.com/articles/ncomms12904>.
- [45] B. A. Bernevig, T. L. Hughes, and S.-C. Zhang, *Science* **314**, 1757 (2006), ISSN 0036-8075, URL <https://www.science.org/doi/10.1126/science.1133734>.
- [46] B. Gharekhanlou and S. Khorasani, in *Graphene: Properties, Synthesis and Application* (Nova Science Publishers, 2011), pp. 1–36, URL <https://link.springer.com/article/10.1007/s11837-022-05505-8>.
- [47] C. Wu and S. Das Sarma, *Physical Review B* **77**, 235107 (2008), ISSN 1098-0121, URL <https://link.aps.org/doi/10.1103/PhysRevB.77.235107>.
- [48] G. W. Semenoff, *Journal of Mathematical Physics* **64**, 071902 (2023), ISSN 0022-2488, URL <https://doi.org/10.1063/5.0135165>.
- [49] T. S. Gardenier, J. J. van den Broeke, J. R. Moes, I. Swart, C. Delerue, M. R. Slot, C. M. Smith, and D. Vanmaekelbergh, *ACS Nano* **14**, 13638 (2020), ISSN 1936-0851, URL <https://pubs.acs.org/doi/10.1021/acsnano.0c05747>.
- [50] S. Chahal, A. Bandyopadhyay, C.-S. Yang, and P. Kumar, *npj 2D Materials and Applications* **7**, 55 (2023), ISSN 2397-7132, URL <https://www.nature.com/articles/s41699-023-00415-y>.
- [51] L. Song, L. Zhang, Y. Guan, J. Lu, C. Yan, and J. Cai, *Chinese Physics B* **28**, 037101 (2019), ISSN 1674-1056, URL <https://iopscience.iop.org/article/10.1088/1674-1056/28/3/037101>.
- [52] R. Stumpf, J. Hannon, and E. Plummer, Tech. Rep., Department of Energy, United States (1994), URL <https://www.osti.gov/biblio/10117200>.
- [53] M. Takahashi, *Scientific Reports* **13**, 13182 (2023), ISSN 2045-2322, URL <https://www.nature.com/articles/s41598-023-40481-2>.
- [54] T. T. Xu, J.-G. Zheng, A. W. Nicholls, S. Stankovich, R. D. Piner, and R. S. Ruoff, *Nano Letters* **4**, 2051 (2004), ISSN 1530-6984, URL <https://pubs.acs.org/doi/10.1021/nl10486620>.
- [55] H. Wang, C. Pan, S.-Y. Wang, H. Jiang, Y.-C. Zhao, Y.-H. Su, G.-H. Zhong, and C. Zhang, *International Journal of Modern Physics C* **32**, 2150057 (2021), ISSN 0129-1831, URL <https://www.worldscientific.com/doi/abs/10.1142/S0129183121500571>.